UDC 55.09.33
https://doi.org/10.17073/0021-3438-2023-5-57-68

Research article
Научная статья

Investigation into the impact of phase composition on the thermal expansion and mechanical properties of Al–Cu–Li alloys

A.A. Ashmarin[1], M.I. Gordeeva[2], S.Ya. Betsofen[2], A.A. Lozovan[2], R. Wu[3], S.S. Alexandrova[2], A.A. Selivanov[4], A.N. Bykadorov[2], D.A. Prokopenko[2]

[1] **Institute of Metallurgy and Materials Science n.a. A.A. Baikov of the Russian Academy of Sciences**
49 Leninskiy Prosp., Moscow, 119334, Russia

[2] **Moscow Aviation Institute (National Research University)**
4 Volokolamskoe Highway, Moscow, 125993, Russia

[3] **Harbin Engineering University**
145 Nantong Str., Harbin 150001, P.R. China

[4] **All-Russian Research Institute of Aviation Materials of the National Research Center "Kurchatov Institute"**
17 Radio Str., Moscow, 105005, Russia

✉ Sergey Ya. Betsofen (s.betsofen@gmail.com)

Abstract: The study employed high-temperature *X*-ray diffraction, quantitative phase analysis, and tensile mechanical property measurements to investigate the relationship between thermal coefficient of linear expansion (TCLE) and phase composition, along with the average yield strengths and Young's moduli of Al–Cu–Li alloys in three different sheet orientations: 1441, V-1461, V-1469, V-1480, and V-1481. The copper content within the solid solution and the mass fractions of the $T_1(Al_2CuLi)$ and $\delta'(Al_3Li)$ phases were determined using an innovative technique based on measuring the lattice distance of the α solid solution, Vegard's law, and balance equations for the elemental and phase compositions of the alloys. It was observed that as the lithium-to-copper ratio in the alloys increased from 0.32 to 1.12, the proportion of the $\delta'(Al_3Li)$ phase increases from 6.3–8.4 wt.% in V-1481, V-1480 and V-1469 alloys to 16.0–17.3 wt.% in 1441 and V-1461 alloys, accompanied by a decrease in the $T_1(Al_2CuLi)$ phase from 5 to 1 wt.%. This led to an increase in the Young's modulus from 75 to 77 GPa due to higher overall proportion of intermetallic compounds and a reduction in yield strength from 509 to 367 MPa due to the decrease in the T_1 phase. This decrease in yield strength resulted from the fact that the hardening effect of the T_1 phase was 3–4 times greater than that of the δ' phase, and this couldn't be offset by an increase in the total intermetallic compound proportion. The observed increase in Young's modulus indicated that the elastic properties of the intermetallic phases were similar, and the rise in the total fraction of intermetallic compounds compensated for the decrease in the T_1 phase. Furthermore, it was demonstrated that TCLE, as measured based on the thermal expansion of the solid solution, also depended on the characteristics of the intermetallic phases present in the alloy. This expanded the potential interpretations of TCLE measurement results.

Keywords: Al–Cu–Li alloys, quantitative phase analysis, high temperature radiography, TCLE, Young's modulus, yield strength.

Acknowledgments: This work received support from the Russian Science Foundation (Grant No. 23-49-00098) and the National Natural Science Foundation of China (52261135538).

For citation: Ashmarin A.A., Gordeeva M.I., Betsofen S.Ya., Lozovan A.A., Wu R., Alexandrova S.S., Selivanov A.A., Bykadorov A.N., Prokopenko D.A. Investigation into the impact of phase composition on the thermal expansion and mechanical properties of Al–Cu–Li alloys. *Izvestiya. Non-Ferrous Metallurgy.* 2023;29(5):57–68. https://doi.org/10.17073/0021-3438-2023-5-57-68

Исследование влияния фазового состава на термическое расширение и механические свойства сплавов Al–Cu–Li

А.А. Ашмарин[1], М.И. Гордеева[2], С.Я. Бецофен[2], А.А. Лозован[2], R. Wu[3], С.С. Александрова[2], А.А. Селиванов[4], А.Н. Быкадоров[2], Д.А. Прокопенко[2]

[1] **Институт металлургии и материаловедения им. А.А. Байкова РАН**
119334, Россия, г. Москва, Ленинский пр-т, 49

[2] **Московский авиационный институт (национальный исследовательский университет)**
125993, Россия, г. Москва, Волоколамское шоссе, 4

[3] **Harbin Engineering University**
P.R. China, 150001, Harbin, Nantong Str., 145

[4] **Всероссийский научно-исследовательский институт авиационных материалов Национального исследовательского центра «Курчатовский институт»**
105005, Россия, г. Москва, ул. Радио, 17

✉ Сергей Яковлевич Бецофен (s.betsofen@gmail.com)

Аннотация: Методами высокотемпературной рентгенографии, количественного фазового анализа и измерения механических свойств при растяжении определяли корреляционные соотношения характеристик термического коэффициента линейного расширения (ТКЛР) и фазового состава с усредненными значениями по 3-м направлениям в листах пределов текучести и модулей Юнга сплавов системы Al–Cu–Li: 1441, В-1461, В-1469, В-1480 и В-1481. Содержание меди в твердом растворе и массовые доли фаз $T_1(Al_2CuLi)$ и $\delta'(Al_3Li)$ оценивали с помощью оригинальной методики, основанной на измерении периода решетки α-твердого раствора, законе Вегарда и уравнениях баланса элементного и фазового составов сплавов. Показано, что с увеличением отношения лития к меди в сплавах от 0,32 до 1,12 повышается доля $\delta'(Al_3Li)$-фазы от 6,3–8,4 мас.% в сплавах В-1481, В-1480 и В-1469 до 16,0–17,3 мас.% в сплавах 1441 и В-1461 за счет снижения количества $T_1(Al_2CuLi)$-фазы от 5 до 1 мас.%. Это приводит к увеличению модуля Юнга от 75 до 77 ГПа из-за возрастания суммарной доли интерметаллидов и к снижению предела текучести от 509 до 367 МПа из-за уменьшения количества T_1-фазы, поскольку эффект упрочнения T_1-фазы в 3–4 раза превосходит упрочнение от выделения δ'-фазы, что не может быть скомпенсировано повышением суммарной доли интерметаллидов. Тот факт, что модуль Юнга при этом увеличивается, свидетельствует о том, что упругие свойства интерметаллидных фаз близки и возрастание суммарной доли интерметаллидов компенсирует снижение количества T_1-фазы. Показано, что величина ТКЛР, измеренная на основании термического расширения твердого раствора, зависит также от характеристик присутствующих в сплаве интерметаллидных фаз, что расширяет возможности интерпретации результатов измерения ТКЛР.

Ключевые слова: сплавы Al–Cu–Li, количественный фазовый анализ, высокотемпературная рентгенография, ТКЛР, модуль Юнга, предел текучести.

Благодарности: Работа выполнена при финансовой поддержке Российского научного фонда (грант № 23-49-00098) и Китайского фонда естественных наук (52261135538).

Для цитирования: Ашмарин А.А., Гордеева М.И., Бецофен С.Я., Лозован А.А., Wu R., Александрова С.С., Селиванов А.А., Быкадоров А.Н., Прокопенко Д.А. исследование влияния фазового состава на термическое расширение и механические свойства сплавов Al–Cu–Li. *Известия вузов. Цветная металлургия.* 2023;29(5):57–68. https://doi.org/10.17073/0021-3438-2023-5-57-68

Introduction

The thermal coefficient of linear expansion (TCLE) is a critical characteristic for both structural and functional materials. A mismatch in TCLE between phases or components can result in product failure during thermal cycling. Additionally, in materials with non-cubic lattices, TCLE anisotropy becomes a significant concern, potentially leading to inconsistent deformation in grains of different orientations, even within single-phase alloys. Experimental determination of TCLE through high-temperature *X*-ray imaging, as opposed to dilatometry, offers the advantage of measuring TCLE in various phases within multiphase systems [1],

as well as in thin surface layers and coatings [2]. However, when it comes to structural materials, research predominantly focuses on determining TCLE values using the dilatometric method, primarily to address component compatibility issues in composite materials.

It is worth noting that many articles in the field of materials science often use the term "thermal expansion" instead of TCLE, emphasizing the physical aspects rather than solely the engineering considerations of these effects. Several studies in this domain delve into the unique category of modern materials characterized by negative (negative thermal expansion — NTE) or small positive (low positive thermal expansion — PTE) thermal expansion [3—5]. This phenomenon is achieved due to the strong anisotropy of interatomic bonding forces, causing TCLE to be negative along some crystallographic directions and positive along others. Consequently, the volumetric TCLE within a certain temperature range is considered as zero thermal expansion ($<1\cdot10^{-6}$ K^{-1}). This effect has been observed in materials such as CrB_2 [3], $Hf_{0.80}Ta_{0.20}Fe_{2.5}$ [4], $Nb_{14}W_3O_{44}$ [5].

This effect is most pronounced in graphite, where the combination of negative TCLE values within the plane of the basis and high positive TCLE values along the "*c*" axis results in significant stress at the interfaces of crystallites with different orientations during thermal cycling. This stress leads to premature material failure. To address this issue, the use of isotropic, isostatically molded graphite has been proposed [6]. Furthermore, research has shown that TCLE anisotropy can be mitigated by utilizing nanographite in the form of carbon nanowalls [7].

In another study [8], the influence of temperature ranging from 25 to 1150 °C on the phase and structural state of NiCrAlY coatings obtained through plasma sputtering was investigated using high-temperature *X*-ray diffraction. This research provided insights into the conditions of metallic and intermetallic phases (γ-Ni, γ′-Ni_3Al, β-NiAl and α-Cr), but also on the oxidation of the coating, including the formation of thermally growing oxides (TGO).

In [9], an innovative approach was proposed to enhance the fracture toughness of α-Al_2O_3 ceramics. This involved creating a layered composite with alternating textureless and textured layers, each characterized by different TCLE values. The authors attributed the improved fracture resistance of the layered composite to the stress state controlled by the TCLE gradient, which holds promise for enhancing the plastic characteristics of ceramics.

For efficient cooling systems with high heat dissipation capacity, a W—Cu composite was developed [10]. This composite combines the high thermal conductivity of Cu with a reduced TCLE ($\sim10\cdot10^{-6}$ K^{-1}) due to the presence of W. This reduction in TCLE makes it compatible with the TCLE of electronic components. High-temperature synchrotron radiation was employed to determine TCLE, including the anisotropy of TCLE, of tetragonal lattice anatase nanoparticles doped with Al, In, In + Cr, and Ag + Cr [11]. Additionally, first-principles TCLE calculations were performed, showing good agreement with experimental data for Cu (isotropic case) and AlN (anisotropic case) [12].

Unfortunately, there is limited literature focusing on the use of thermal expansion for metallurgical purposes. While magnesium alloys offer several advantages, their high TCLE ($26\cdot10^{-6}$ K^{-1}), restricts their use in electronics. Consequently, research is actively exploring alloying elements that can reduce the TCLE of magnesium [13—15]. For example, a study demonstrated that the addition of 4 wt.% Si reduces the TCLE of pure Mg from $26\cdot10^{-6}$ to $17.98\cdot10^{-6}$ K^{-1} due to the formation of the Mg_2Si phase with a low TCLE value of $7{,}5\cdot10^{-6}$ K^{-1}. In the case of VNS9-Sh TRIP steel, research [16] revealed a decomposition of approximately 40 % of austenite within a surface layer of about 5 μm, resulting in significant compressive stresses. To understand these processes in thin layers, determining TCLE values of α and γ phases in TRIP steel under different thermomechanical conditions is crucial [17].

A promising approach for analyzing multiphase systems is demonstrated in a study [1], where TCLE measurements of solid solutions, silicon, and six intermetallic phases in foundry alloys such as Al—9.5Si—5.1Cu—0.5Fe, Al—12.5Si—3.9Cu—2.8Ni—0.7Mg—0.4Mn, Al—9.6Si—4.4Ni—0.5Fe, Al—9.5Si—2.5Mn—0.5Fe were conducted using high-temperature *X*-ray radiography (from room temperature to 400 °C). Importantly, the alloy compositions were carefully selected to ensure distinct diffraction from intermetallic compounds, enabling the determination of TCLE values along different crystallographic axes of tetragonal Al_2Cu, monoclinic Al_9FeNi, hexagonal Al_3Ni_2, orthorhombic Al_3Ni, and trigonal Al_7Cu_4Ni. This allowed for the identification of correlations not only related to the mismatch between TCLE values of intermetallic compounds and the matrix but also to their anisotropy. The results from this study [1] highlight that TCLE compatibility issues are relevant not only for substrate coatings and composite

components but also for solid solutions and intermetallic particles. Moreover, investigating the relationships between TCLE values and the mechanical and service properties of alloys and coatings is of great importance.

Al—Li alloys are extensively utilized in aerospace applications owing to their unique blend of low density, necessary strength, and exceptionally high elastic modulus values in comparison to other aluminum alloys [18]. Currently, research is advancing in the direction of developing a new generation of materials for aircraft construction: laminated aluminous-glass plastics (SIALs) based on the Al—Cu—Li system. This innovation is projected to enhance the elastic modulus by 8—10 % while reducing the density of SIALs by 5—7 % [19; 20]. Nevertheless, optimizing alloy compositions to achieve maximum strength or elastic properties encounters methodological challenges in estimating elastic properties. In this context, exploring correlations between the elastic moduli and TCLE values of Al—Cu—Li alloys holds promise.

This paper examines the relationships between TCLE characteristics and the properties of Al—Cu—Li alloys. Such investigations can broaden the applicability of the TCLE measurement method concerning the study and prediction of the structural phase state and properties of these materials.

1. Materials and methods

1.1. Materials

The materials employed in this study comprised sheets of Al—Cu—Li alloys with thicknesses ranging from 1 to 3 mm. Specifically, the alloys examined included 1441, V-1461, V-1469, V-1480, and V-1481 variants. Table 1 provides the composition details of the primary alloying elements (Cu and Li). These sheets were manufactured through rolling processes at OAO "KUMZ" (Kamensk—Uralsky). Subsequently, they underwent a series of heat treatments, including: hardening via cooling in cold water, straightening, and artificial ageing with either, two, or three stages. Al—Li alloy samples were tested using a Zwick/Roell KAPPA 50DS testing machine (Germany) equipped with a force sensor of accuracy class 0.5 and a makroXtens strain gauge (Zwick Roell, Germany) with a 50 mm design length. The testing procedure began with a motion speed of 2 mm/min in the elastic segment, which was subsequently increased to 5 mm/min once the yield strength was determined. Tensile mechanical properties at room temperature were determined according to State Standards GOST 1497 and GOST 11701, and Young's modulus was calculated using regression analysis on a linear segment.

1.2. Methods

X-ray diffraction patterns were recorded using an XRD-600 *X*-ray diffractometer (Shimadzu, Japan) with a HA-1001 high-temperature attachment in an atmospheric environment. Copper radiation was employed with β filtering, and data were collected in the angular range $2\theta = 20 \div 60°$ at temperatures of 20, 100, 150, 200, 300, 400, 500 °C.

In order to determine the lattice period (a) for the reflection (hkl) of a crystal with a cubic lattice at each recording temperature (t_i), the following formula was applied:

$$a_{t_i} = [\lambda/(2\sin\theta)]\sqrt{h^2 + k^2 + l^2}. \quad (1)$$

The TCLE values ($\alpha_{100-500}$) were calculated for the temperature range of 100—500 °C by the least squares method by determining the slope of the straight line in the corresponding coordinates $a_{t_i} - t_i$ (Fig. 1).

2. Results and discussion

Figure 2 illustrates *X*-ray diffraction patterns for five alloys within the Al—Cu—Li system, each distinguished by variations in their Cu and Li content.

These *X*-ray diffraction patterns exclusively display reflections from the FCC α solid solution. Neverthe-

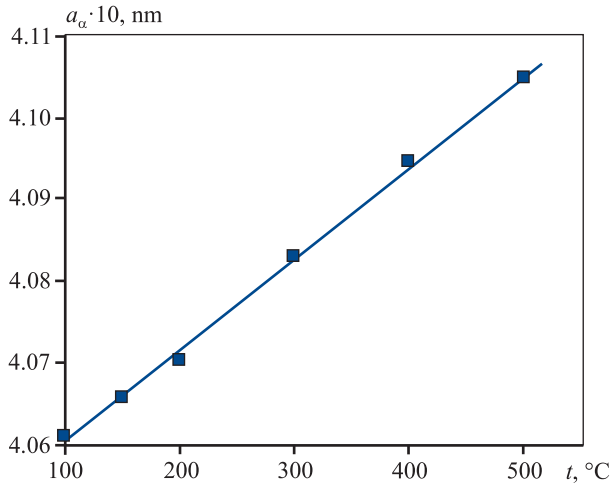

Fig. 1. Lattice distance as a function of *X*-ray temperature for the (111) reflection of the V-1469 alloy

Рис. 1. Зависимость периода решетки от температуры рентгеновской съемки для рефлекса (111) сплава В-1469

less, the relative intensities of these reflections differ across the various alloys. This discrepancy in reflection intensities hints at differences in textures, which play a vital role in explaining the inherent anisotropy of properties characteristic of alloys within this alloying system.

By calculating the lattice periods of the α solid solution based on the position of the reflections in the *X*-ray diffraction patterns, it becomes possible to estimate the copper content within the solid solution and the mass fractions of the $T_1(Al_2CuLi)$ and $\delta'(Al_3Li)$ phases. This estimation is carried out using an innovative technique, as described in [21]. The method relies on measuring the lattice period of an α solid solution, applying Vegard's law, and employing balance equations for the elemental and phase compositions of these alloys. The calculation

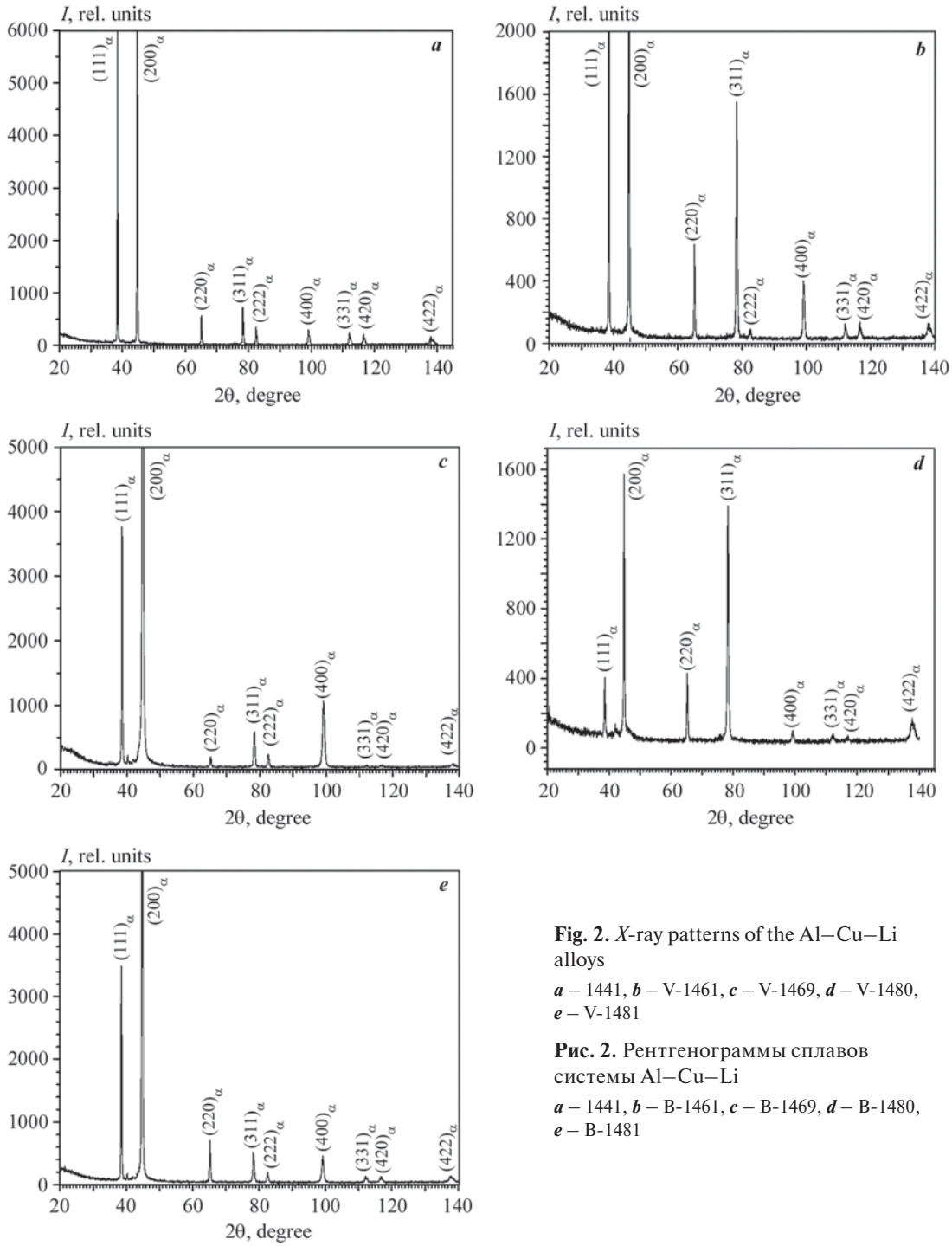

Fig. 2. *X*-ray patterns of the Al–Cu–Li alloys

a – 1441, ***b*** – V-1461, ***c*** – V-1469, ***d*** – V-1480, ***e*** – V-1481

Рис. 2. Рентгенограммы сплавов системы Al–Cu–Li

a – 1441, ***b*** – B-1461, ***c*** – B-1469, ***d*** – B-1480, ***e*** – B-1481

equations for alloys of the Al—Cu—Li system are as follows:

$$W_\alpha = \left[(X^{\delta'}_{Li} - X^{T_1}_{Li})(X^0_{Al}X^{T_1}_{Cu} - X^{T_1}_{Al}X^0_{Cu}) - \right.$$
$$\left. - X^{\delta'}_{Al}X^{T_1}_{Cu}(X^0_{Li} - X^{T_1}_{Li})\right] /$$
$$/ \left[(X^{\delta'}_{Li} - X^{T_1}_{Li})(100X^{T_1}_{Cu} - X^{\alpha}_{Cu}X^{T_1}_{Cu} - X^{T_1}_{Cu}X^{\alpha}_{Li} - X^{T_1}_{Al}X^{\alpha}_{Cu}) - \right.$$
$$\left. - X^{\delta'}_{Al}X^{T_1}_{Cu}(X^{\alpha}_{Li} - X^{T_1}_{Li})\right] \cdot 100,$$

$$W_{T_1} = \frac{100X^0_{Cu} - X^{\alpha}_{Cu}W_\alpha}{X^{T_1}_{Cu}}, \quad (2)$$

$$W_{\delta'} = 100 - W_\alpha - W_{T_1},$$

where X^0_{Al}, X^0_{Cu}, X^0_{Li} represent the concentrations of Al, Cu and Li in the alloy, respectively, wt.%; W_α, W_{T_1}, $W_{\delta'}$ denote the content of the α, T_1 and δ′ phases, respectively, wt.%; X^{α}_{Al}, X^{α}_{Cu}, X^{α}_{Li}, $X^{T_1}_{Al}$, $X^{T_1}_{Cu}$, $X^{T_1}_{Li}$, $X^{\delta'}_{Al}$, $X^{\delta'}_{Li}$ represent the concentrations of Al, Cu and Li in the α, T_1 and δ′ phases, respectively.

The values of $X^{\delta'}_{Li}$, $X^{\delta'}_{Al}$, $X^{T_1}_{Al}$, $X^{T_1}_{Cu}$, $X^{T_1}_{Li}$ are calculated based on the stoichiometry of the $T_1(Al_2CuLi)$ and δ′(Al_3Li) phases.

$$X^{\alpha}_{Cu} = \frac{a_\alpha - a_{Al} - 0{,}01W_\alpha X^0_{Mg}(\Delta a/\Delta X)^{\alpha}_{Mg}}{(\Delta a/\Delta X)^{\alpha}_{Cu}},$$

$0{,}01W_\alpha X^0_{Mg}(\Delta a/\Delta X)^{\alpha}_{Mg}$ is the change in the lattice constant due to presence of magnesium in the solid solution, Å; $(\Delta a/\Delta X)^{\alpha}_{Cu}$ represents the change of the lattice constant by 1 wt.% Cu, Å/wt.%.

Figure 3 provides graphical representations of the dependencies of mass fractions of intermetallic phases for two of the five alloys, specifically 1441 and V-1480. These dependencies reveal a clear trend: as the ratio of lithium content to copper content in the alloy increases, the fraction of the δ′ phase markedly rises, while the fraction of the ternary phase decreases. Table 1 compiles the quantities of intermetallic phases, calculated using Eq. (2), further confirming this pattern.

The ratio X^0_{Li}/X^0_{Cu} increases from 0.32 in the V-1480 alloy to 1.12 in the 1441 alloy. This increase in this ratio results in a higher fraction of the δ′(Al_3Li) phase, ranging from 6.3 to 17.3 wt.%, while reducing the proportion of the $T_1(Al_2CuLi)$ phase from 5 to 1 wt.%. Consequently, the total amount of intermetallic phases increases because the δ′ phase (6.3—17.3 wt.%) significantly outweighs the T_1 phase (1—5 wt.%) in quantity. It is noteworthy that the total amount of intermetallic phases in these alloys is notably greater than in other aluminum alloys. Only in the V-1481 alloy, with a low lithium content of 1 wt.%, does the total amount of intermetallic phases fall below 10 wt.% (7.5 wt.%). In the remaining four alloys, the quantity of intermetallic compounds ranges from 11.7 to 18.5 wt.%. This observation accounts for the fact that alloys containing lithium exhibit the highest Young's modulus among aluminum alloys.

Another notable characteristic of these alloys is the significantly more pronounced anisotropy in mechanical properties when compared to other aluminum alloys. Interestingly, the crystallographic texture in alloys con-

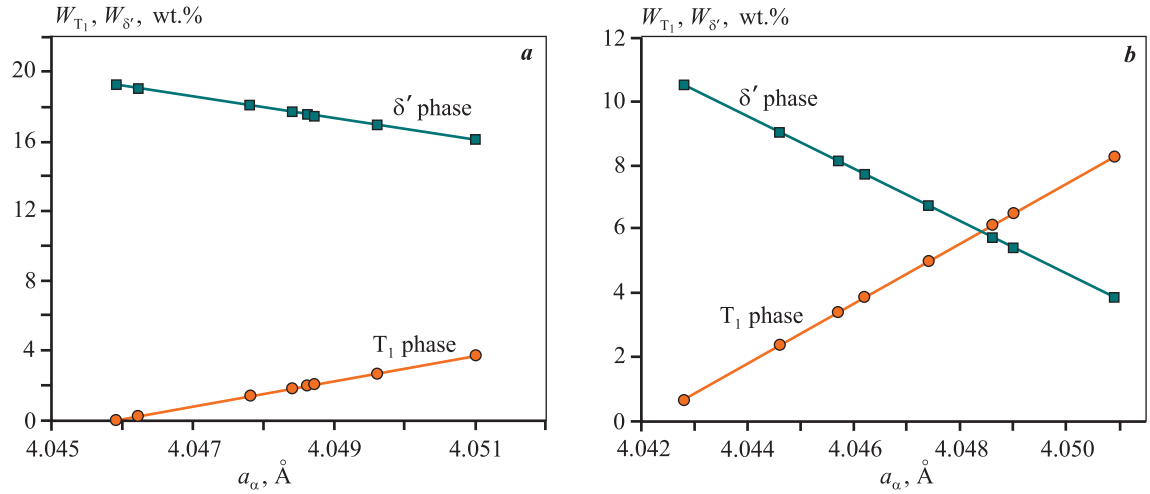

Fig. 3. Fractions of T_1 and δ′ phases as a function of the lattice period of the α-Al-solid solution in Al–Cu–Li alloys
a – alloy 1441 (1.6Cu–1.8Li); ***b*** – V-1480 (3.8Cu–1.2Li)

Рис. 3. Зависимости количества T_1 и δ′-фаз от периода решетки α-твердого раствора Al в сплавах системы Al–Cu–Li
a – сплав 1441 (1,6Cu–1,8Li); ***b*** – В-1480 (3,8Cu–1,2Li)

Table 1. **Primary alloying elements (Cu and Li), wt.%, and content of T_1 and δ′ phases, wt.%, within Al–Cu–Li alloys**

Таблица 1. Количество основных легирующих элементов (Cu и Li), мас.%, и содержание T_1- и δ′-фаз, мас.%, в сплавах системы Al–Cu–Li

Alloy	X^0_{Cu}	X^0_{Li}	X^0_{Li}/X^0_{Cu}	W_{T_1}	$W_{\delta'}$	$W_{T_1} + W_{\delta'}$
V-1480	3.8	1.2	0.32	5.0	6.7	11.7
V-1481	3.0	1.0	0.33	1.2	6.3	7.5
V-1469	3.8	1.3	0.34	4.6	8.4	13.0
V-1461	2.9	1.8	0.62	2.5	16.0	18.5
1441	1.6	1.8	1.12	1.0	17.3	18.3

Table 2. **Primary alloying elements (Cu and Li), TCLE (α), Young's modulus (*E*) and yield strength ($\sigma_{0.2}$) within Al–Cu–Li alloys**

Таблица 2. Количество основных легирующих элементов (Cu и Li), величины ТКЛР (α), модуля Юнга (*E*) и предела текучести ($\sigma_{0,2}$) в сплавах системы Al–Cu–Li

Alloy	X^0_{Cu}, wt.%	X^0_{Li}, wt.%	X^0_{Li}/X^0_{Cu}	$\alpha \cdot 10^6$, K^{-1}	*E*, GPa	$\sigma_{0,2}$, MPa
V-1480	3.8	1.2	0.32	26.2	75.3	509.2
V-1481	3.0	1.0	0.33	26.0	75.1	478.8
V-1469	3.8	1.3	0.34	25.1	74.5	509.2
V-1461	2.9	1.8	0.62	23.6	76.5	468.3
1441	1.6	1.8	1.12	22.8	77.3	366.7

taining lithium is practically indistinguishable from that in other aluminum alloys. It is possible that intermetallic phases play a role in contributing to this anisotropy effect. Investigating the anisotropy of these alloys is a distinct endeavor and will be the focus of our upcoming study. The current research aims to establish correlations between chemical and phase compositions, mechanical properties, and thermal expansion in lithium-containing alloys. Given the complexity of accounting for anisotropy, we opted to average the mechanical properties using a well-known formula for estimating the Lankford coefficient, which is averaged for sheet materials:

$$X_{avg} = (X_L + X_T + 2X_{45°})/4, \quad (3)$$

where $X = E$, σ_u, $\sigma_{0.2}$, δ are in the longitudinal rolling direction (L), transversal direction (T), and at an angle of 45°.

Figure 4, which illustrates the anisotropy of mechanical properties, showcases the results of testing in three directions for the V-1480 alloy sheet. The mechanically averaged properties, calculated using Eq. (3), are presented in Table. 2.

The increase in the X^0_{Li}/X^0_{Cu} ratio from 0.32 in alloy V-1480 to 1.12 in alloy 1441 is accompanied by a rise in Young's modulus and a decline in yield strength of these alloys (Fig. 5, *a*). However, the underlying reasons for these changes differ. The increase in Young's modulus is attributed to a rise in the overall proportion of intermetallic compounds, progressing from 7.5—13.0 wt.% in V-1481, V-1480, and V-1469 alloys to 18.3—18.5 wt.% in 1441 and V-1461 alloys (see Table 1). Conversely, the quantity of the T_1 phase decreases, contributing to a reduction in yield strength (Fig. 5, *b*). This decrease in yield strength occurs because, as demonstrated in [21], the hardening effect caused by the T_1 phase is 3—4 times greater than the hardening effect resulting from δ′ phase separation. Consequently, the decrease in the amount of the T_1 phase in 1441 and V-1461 alloys cannot be adequately offset by a significant increase in the overall proportion of intermetallic compounds in these alloys. The fact that Young's modulus increases while yield strength decreases indicates that the elastic properties of the intermetallic phases are comparable, and the overall increase in the fraction of intermetallic compounds compensates for the decrease in the T_1 phase content.

Figure 6 displays the composite *X*-ray diffraction images of the (200) planes of the α Al solid solution for alloys 1441 and V-1469. These images were acquired through imaging at temperatures of 20, 100, 200, 300, 400, and 500 °C. These images were then used to cal-

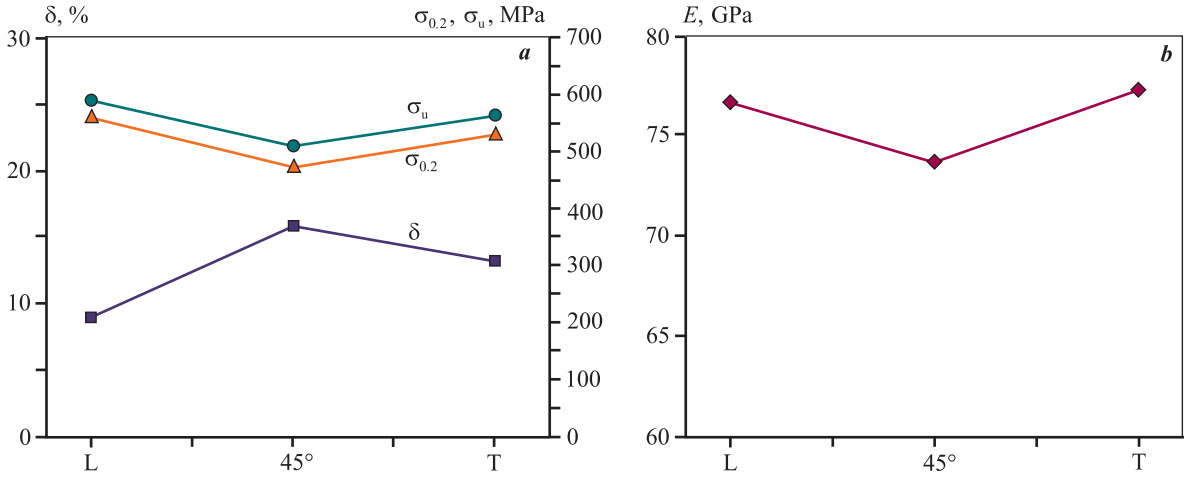

Fig. 4. Mechanical properties (δ, $\sigma_{0.2}$, σ_u, *E*) of V-1480 alloy sheets in the longitudinal rolling direction (L), transverse direction (T) and at a 45°angle

Рис. 4. Механические свойства (δ, $\sigma_{0,2}$, $\sigma_в$, *E*) листов сплава В-1480 в долевом направлении прокатки (L), поперечном (Т) и под углом 45°

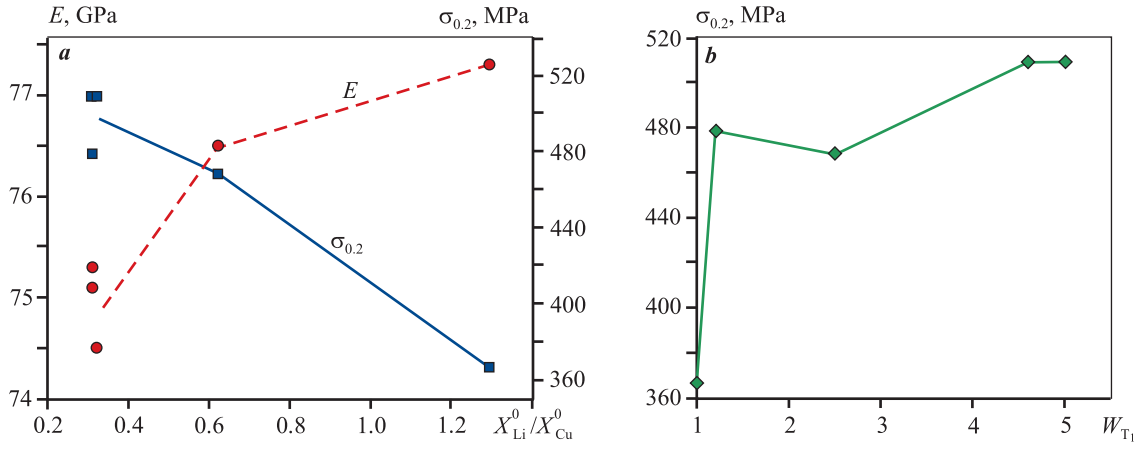

Fig. 5. Young's modulus and yield strength as functions of the ratio of lithium to copper concentration (X^0_{Li}/X^0_{Cu}) (***a***), and yield strength as a function of the amount of T_1-phase (***b***) in Al–Cu–Li alloys

Рис. 5. Зависимости модуля Юнга и предела текучести от соотношения концентраций лития и меди (X^0_{Li}/X^0_{Cu}) (***a***) и зависимость предела текучести от количества T_1-фазы (***b***) в сплавах системы Al–Cu–Li

culate the TCLE, with the resulting values (α) provided in Table 2.

The rise in the X^0_{Li}/X^0_{Cu} ratio from alloy V-1481 to alloy 1441 coincides with an increase in Young's modulus and a decrease in TCLE (Fig. 7). This pattern would be expected for a single-phase alloy, as an increase in Young's modulus typically signifies an augmentation in interatomic bonding forces, which, in turn, should lead to a reduction in TCLE. However, in the case of alloys containing lithium, the heightened Young's modulus is attributed to the substantial presence of intermetallic phases, which possess a higher Young's modulus than the solid solution. Consequently, the decrease in TCLE value may not be directly attributed to this factor. This is because the TCLE measurement pertains solely to the solid solution and not to the TCLE of the solid solution combined with intermetallic compounds, as is the case with Young's modulus measurements.

Therefore, the variation in TCLE in Al—Cu—Li alloys suggests that TCLE values, measured based on the thermal expansion of the atoms within the solid solution, exhibit a dependency on the intermetallic particles present within the solid solution. This dependency's presence should result in a violation of the additivity rule when averaging TCLE for composites and multiphase alloys comprising components with significantly different elastic properties. The most well-known models

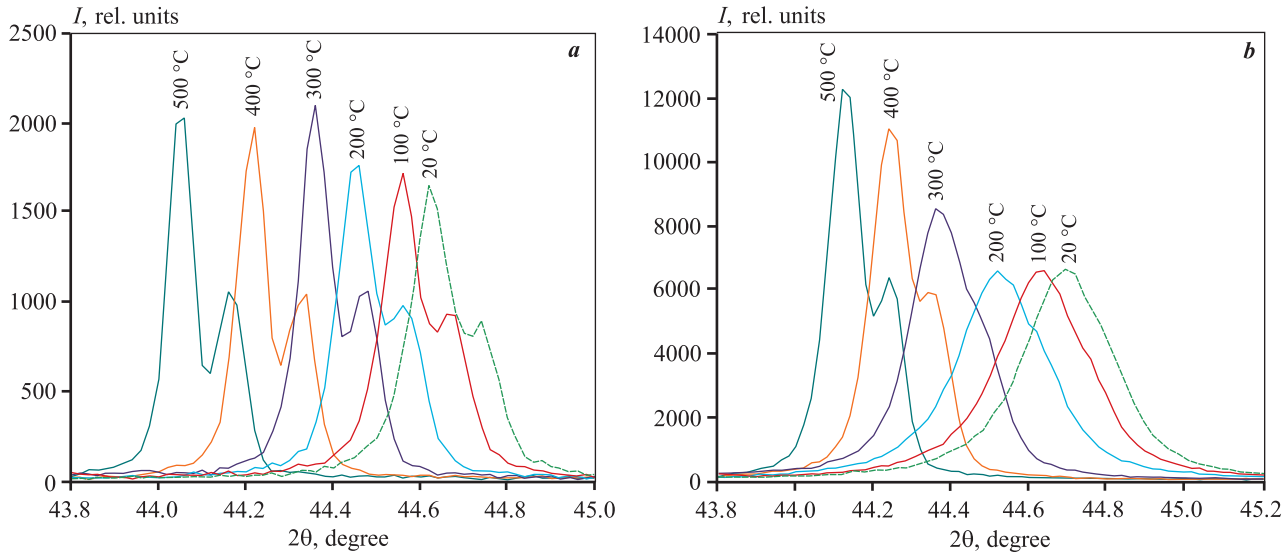

Fig. 6. Combined reflections (200) of the α Al solid solution, obtained by *X*-ray photography of alloys 1441 (***a***) and V-1469 (***b***) at different temperatures

Рис. 6. Совмещенные рефлексы (200) α-твердого раствора Al, полученные рентгеновской съемкой сплавов 1441 (***a***) и В-1469 (***b***) при различных температурах

for such averaging are the Kerner model (Eq. 4) and the Turner model (Eq. 5):

$$\alpha = \alpha_m - (\alpha_m - \alpha_p) \times$$

$$\times \frac{K_p(3K_m + 4G_m)V_p}{K_m(3K_p + 4G_m) + 4(K_p - K_m)G_m V_p}, \quad (4)$$

$$\alpha = \frac{\alpha_m K_m V_m + \alpha_p K_p V_p}{K_m V_m + K_p V_p}, \quad (5)$$

where $K = E/[3(1 - 2\nu)]$ represents the volumetric modulus, $G = E/[2(1 + \nu)]$ denotes the shear modulus, V_m and V_p represent the volumetric fractions of the matrix and the second phase, respectively. These models were employed in [13] during studies involving the influence of Si on TCLE of Mg—Si—Ca alloys. The results demonstrated that the experimental TCLE values align with the calculations within the framework of the Kerner model. These findings underscore the complex nature of the interaction between the matrix and the second phase during thermal expansion.

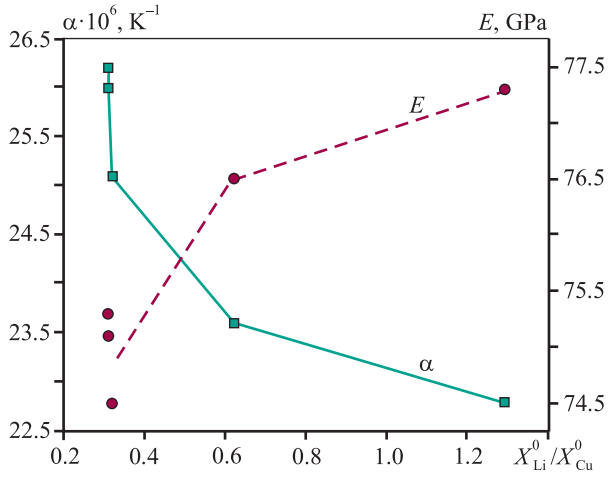

Fig. 7. Dependence of TCLE (α) and Young's modulus (*E*) as a function of the ratio of lithium to copper concentration (X^0_{Li}/X^0_{Cu}) for Al–Cu–Li alloys

Рис. 7. Зависимость ТКЛР (α) и модуля Юнга (*E*) от соотношения концентраций лития и меди (X^0_{Li}/X^0_{Cu}) для сплавов системы Al–Cu–Li

Conclusions

An analysis was conducted to examine the correlation between thermal coefficient of linear expansion (TCLE) characteristics and phase composition with the properties of Al—Cu—Li alloys under tensile stress. The study reveals that an increase in the ratio of lithium to copper content in the alloys results in a higher proportion of the δ′(Al_3Li) phase, primarily due to a decrease in the quantity of the T_1(Al_2CuLi) phase. Additionally, the overall amount of intermetallic phases increases because the δ′ phase significantly outweighs the T_1 phase in quantity. This leads to an increase in Young's modulus but a decrease in yield strength and TCLE. The rise in Young's modulus is attributed to the increased presence of intermetallic compounds, while the decline in yield

strength is associated with the decreased T_1 phase content. It's worth noting that the hardening effect of the T_1 phase is 3—4 times greater than that of the δ′ phase, and a reduction in the T_1 phase content cannot be fully compensated by an increase in the overall fraction of intermetallic compounds. The fact that Young's modulus increases while yield strength decreases indicates that the elastic properties of the intermetallic phases are similar. Consequently, the overall increase in the fraction of intermetallic compounds compensates for the decrease in the T_1 phase content. The study demonstrates that TCLE, measured based on the thermal expansion of solid solution atoms, is influenced by the characteristics of the intermetallic phases present in the alloy. This suggests that TCLE in multiphase alloys and composites results from a complex interaction among mixture components. While this complexity complicates the interpretation of TCLE measurements, it also broadens the possibilities for interpretations.

References

1. Saringer C., Kickinger C., Munnik F., Schalk N., Tkadletz M. Thermal expansion of magnetron sputtered TiC_xN_{1-x} coatings studied by high-temperature *X*-ray diffraction. *Thin Solid Films*. 2019;688:137307. https://doi.org/10.1016/j.tsf.2019.05.026
2. Chen C.-L., Thomson R.C. Study on thermal expansion of intermetallics in multicomponent Al—Si alloys by high temperature *X*-ray diffraction. *Intermetallics*. 2010;18(9):1750—1757. https://doi.org/10.1016/j.intermet.2010.05.015
3. Yong Xu, Xin Chen, Yili Cao, Kun Lin, Chin-Wei Wang, Qiang Li, Jinxia Deng, Jun Miao, Xianran Xing. Neutron diffraction study on anomalous thermal expansion of CrB_2. *Chinese Journal of Structural Chemistry*. 2023; (January):100009. https://doi.org/10.1016/j.cjsc.2022.100009
4. Dongyu Cen, Bin Wang, Ruixue Chu, Yuanyuan Gong, Guizhou Xu, Fenghua Chen, Feng Xu. Design of (Hf,Ta)Fe_2/Fe composite with zero thermal expansion covering room temperature. *Scripta Materialia*. 2020;186: 331—335. https://doi.org/10.1016/j.scriptamat.2020.05.048
5. Niu Zhang, Jinghua Li, Xiaoshuai Kong, Mengting She, Peng Guo, Jingjing Sun, Peiling Yuan, Shuaipu Zang, Mingju Chao, Erjun Liang. Negative thermal expansion property in $Nb_{14}W_3O_{44}$. *Journal of Materials Research and Technology*. 2022;18:3841—3848. https://doi.org/10.1016/j.jmrt.2022.04.083
6. Keith R. Hallama, James Edward Darnbrough, Charilaos Paraskevoulakos, Peter J. Hearda, T. James Marrow, Peter E.J.Flewitt. Measurements by *X*-ray diffraction of the temperature dependence of lattice parameter and crystallite size for isostatically-pressed graphite. *Carbon Trends*. 2021;4:100071. https://doi.org/10.1016/j.cartre.2021.100071
7. Kazuma Akikubo, Tyler Kurahashi, Sota Kawaguchi, Masaru Tachibana. Thermal expansion measurements of nano-graphite using high-temperature *X*-ray diffraction. *Carbon*. 2020;169:307—311. https://doi.org/10.1016/j.carbon.2020.07.027
8. Abhijith Vijay V., Santhy K., Sivakumar G., Rajasekaran B. Thermal expansion and microstructure evolution of atmospheric plasma sprayed NiCrAlY bond coat using in-situ high temperature *X*-ray diffraction. *Surface and Coatings Technology*. 2023;452:129132. https://doi.org/10.1016/j.surfcoat.2022.129132
9. Josef Schlacher, Zdenek Chlup, Anna-Katharina Hofer, Raul Bermejo. High-temperature fracture behaviour of layered alumina ceramics with textured microstructure. *Journal of the European Ceramic Society*. 2023;43(7): 2917—2927. https://doi.org/10.1016/j.jeurceramsoc.2022.11.046
10. Huanbei Chen, Feiyu Zheng, Weizheng Cheng, Peng Tao, Chengyi Song, Wen Shang, Benwei Fu, Tao Deng. Low thermal expansion metal composite-based heat spreader for high temperature thermal management. *Materials & Design*. 2021;208:109897. https://doi.org/10.1016/j.matdes.2021.109897
11. Hani Manssor Albetran. Thermal expansion coefficient determination of pure, doped, and co-doped anatase nanoparticles heated in sealed quartz capillaries using in-situ high-temperature synchrotron radiation diffraction. *Heliyon*. 2020;6(7):e04501. https://doi.org/10.1016/j.heliyon.2020.e04501
12. Pikea Nicholas A., Løvvika Ole M. Calculation of the anisotropic coefficients of thermal expansion: A first-principles approach. *Computational Materials Science*. 2019;167:257—263. https://doi.org/10.1016/j.commatsci.2019.05.045
13. Guo Tian, Wu Shusen, Zhou Xiong, Lü Shulin, Xia Lanqing. Effects of Si content and Ca modification on microstructure and thermal expansion property of Mg—Si alloys. *Materials Chemistry and Physics*. 2020;253:123260. https://doi.org/10.1016/j.matchemphys.2020.123260
14. Wang Xue Yi, Yang Jun, Chi Pei Zhou, Bahonar Ehsan, Tayebi Morteza. Effects of the microstructure and precipitation hardening on the thermal expansion behavior of ZK60 magnesium alloy. *Journal of Alloys and Compounds*. 2022;901:163422. https://doi.org/10.1016/j.jallcom.2021.163422
15. Ningning Dong, Jinhui Wang, Hongbin Ma, Peipeng Jin. Effects of Nd content on thermal expansion be-

havior of Mg—Nd alloys. *Materials Today Communication*. 2021;29:102894. https://doi.org/10.1016/j.mtcomm.2021.102894

16. Betsofen S.Y., Ashmarin A.A., Terent'ev V.F., Grushin I.A., Lebedev M.A. Phase composition and residual stresses in the surface layers of VNS9-Sh TRIP steel. *Russian Metallurgy (Metally).* 2020;(11):1129—1136. https://doi.org/10.1134/S0036029520100067
Бецофен С.Я., Ашмарин А.А., Терентьев В.Ф., Грушин И.А., Лебедев М.А. Фазовый состав и остаточные напряжения в поверхностных слоях трип-стали ВНС9-Ш. *Деформация и разрушение материалов*. 2020;6:12—20.
17. Ashmarin A.A., Betsofen S.Y., Lukin E.I. Effect of annealing on the phase composition and the linear thermal expansion coefficient of VNS9-Sh TRIP steel. *Russian Metallurgy (Metally).* 2022;(11):1397—1402. https://doi.org/10.1134/S0036029522110027
Ашмарин А.А., Бецофен С.Я., Лукин Е.И. Исследование влияния отжига на фазовый состав и термические коэффициенты линейного расширения трип-стали ВНС9-Ш. *Металлы*. 2022;6:66—72.
18. Betsofen S.Y., Antipov V.V., Serebrennikova N.Y., Dolgova M.I., Kabanova Yu.A. Phase composition, texture, and anisotropy of the properties of Al—Cu—Li—Mg alloy sheets. *Russian Metallurgy (Metally).* 2017;2017(10):831—837. https://doi.org/10.1134/S0036029517100044
Бецофен С.Я., Антипов В.В., Долгова М.И. Серебренникова Н.Ю., Кабанова Ю.А. Исследование фазового состава, текстуры и анизотропии свойств листов из сплавов системы Al—Cu—Li—Mg. *Деформация и разрушение материалов*. 2017;1:24—30.
19. Kablov E.N., Antipov V.V., Girsh R.I., Serebrennikova N.Yu., Konovalov A.N. Designed layered materials based on sheets of aluminum-lithium alloys and fiberglass in the designs of new generation aircrafts. *Vestnik Mashinostroeniya*. 2020;(12):46—52. (In Russ.). http://dx.doi.org/10.36652/0042-4633-2020-12-46-52
Каблов Е.Н., Антипов В.В., Гирш Р.И., Серебренникова Н.Ю., Коновалов А.Н. Конструируемые слоистые материалы на основе листов из алюминий-литиевых сплавов и стеклопластиков в конструкциях летательных аппаратов нового поколения. *Вестник машиностроения*. 2020;(12):46—52.
20. Kablov E.N., Antipov V.V., Oglodkova Yu.S., Ogladkov M.S. Development and application prospects of aluminum—lithium alloys in aircraft and space technology. *Metallurgist*. 2021;65(1-2):72—81. https://doi.org/10.1007/s11015-021-01134-9
Каблов Е.Н., Антипов В.В., Оглодкова Ю.С., Оглодков М.С. Опыт и перспективы применения алюминий-литиевых сплавов в изделиях авиационной и космической техники. *Металлург.* 2021;65(1):62—70.
21. Betsofen S.Y., Antipov V.V., Grushin I.A., Knyazev M.I., Khokhlatova L.B., Alekseev A.A. Effect of the composition of Al—Li alloys on the quantitative relation between the $\delta'(Al_3Li)$, $S_1(Al_2MgLi)$, and $T_1(Al_2CuLi)$ phases. *Russian Metallurgy (Metally).* 2015;(1):51—58. https://doi.org/10.1134/S0036029515010024
Бецофен С.Я., Антипов В.В., Грушин И.А., Князев М.И., Хохлатова Л.Б., Алексеев А.А. Закономерности влияния состава Al—Li сплавов на количественное соотношение $\delta'(Al_3Li)$, $S_1(Al_2MgLi)$ и $T_1(Al_2CuLi)$ фаз. *Металлы*. 2015;(1):59—66.

Information about the authors

Artem A. Ashmarin – Cand. Sci. (Eng.), Leading Researcher, Institute of Metallurgy and Materials Science n.a. A.A. Baikov of the Russian Academy of Sciences.
https://orcid.org/0000-0003-3160-5179
E-mail: ashmarin_artem@list.ru

Margarita I. Gordeeva – Cand. Sci. (Eng.), Associate Prof., Department 1102, Moscow Aviation Institute (National Research University) (MAI).
https://orcid.org/0009-0003-0538-6926
E-mail: gordeevami@mai.ru

Sergey Ya. Betsofen – Dr. Sci. (Eng.), Professor, Department 1101, MAI.
https://orcid.org/0000-0003-0931-2839
E-mail: s.betsofen@gmail.com

Alexander A. Lozovan – Dr. Sci. (Eng.), Professor, Department 1101, MAI.
https://orcid.org/0000-0001-9478-6793
E-mail: loz-plasma@yandex.ru

Информация об авторах

Артем Александрович Ашмарин – к.т.н., ведущий научный сотрудник Института металлургии и материаловедения им. А.А. Байкова (ИМЕТ) РАН.
https://orcid.org/0000-0003-3160-5179
E-mail: ashmarin_artem@list.ru

Маргарита Игоревна Гордеева – к.т.н., доцент кафедры 1102 Московского авиационного института (национального исследовательского университета) (МАИ).
https://orcid.org/0009-0003-0538-6926
E-mail: gordeevami@mai.ru

Сергей Яковлевич Бецофен – д.т.н., профессор, кафедра 1101 МАИ.
https://orcid.org/0000-0003-0931-2839
E-mail: s.betsofen@gmail.com

Александр Александрович Лозован – д.т.н., профессор, кафедра 1101 МАИ.
https://orcid.org/0000-0001-9478-6793
E-mail: loz-plasma@yandex.ru

Ruizhi Wu – Ph.D, Deputy Head of Key Laboratory, Harbin Engineering University.
E-mail: rzwu@hrbeu.edu.cn

Svetlana S. Alexandrova – Cand. Sci. (Eng.), Associate Prof., Department 1101, MAI.
https://orcid.org/0000-0002-3134-2375
E-mail: sweta.sergeeva@gmail.com

Andrey A. Selivanov – Cand. Sci. (Eng.), Head of the laboratory, All-Russian Research Institute of Aviation Materials of the National Research Center "Kurchatov Institute".
https://orcid.org/0009-0006-0028-1684
E-mail: julies87@mail.ru

Artem N. Bykadorov – Engineer, Department 1101, MAI.
https://orcid.org/0009-0006-9561-7354
E-mail: xartem94@mail.ru

Denis A. Prokopenko – Engineer, MAI.
https://orcid.org/0000-0002-9932-5344
E-mail: denis.prokop1234@gmail.com

Ruizhi Wu – PhD, зам. заведующего ключевой лабораторией Харбинского технического университета.
E-mail: rzwu@hrbeu.edu.cn

Светлана Сергеевна Александрова – к.т.н., доцент, кафедра 1101 МАИ.
https://orcid.org/0000-0002-3134-2375
E-mail: sweta.sergeeva@gmail.com

Андрей Аркадьевич Селиванов – к.т.н., начальник лаборатории, НИЦ «Курчатовский институт»–ВИАМ.
https://orcid.org/0009-0006-0028-1684
E-mail: julies87@mail.ru

Артем Никитич Быкадоров – инженер, кафедра 1101 МАИ.
https://orcid.org/0009-0006-9561-7354
E-mail: xartem94@mail.ru

Денис Алексеевич Прокопенко – инженер МАИ.
https://orcid.org/0000-0002-9932-5344
E-mail: denis.prokop1234@gmail.com

Contribution of the authors

A.A. Ashmarin – conducted *X*-ray phase analysis.

M.I. Gordeeva – participated in the discussion of the results.

S.Ya. Betsofen – contributed to the discussion of the results, and drafted the manuscript.

A.A. Lozovan – formulated the research objectives, contributed to the discussion of the results, and co-wrote the manuscript.

R. Wu – participated in the discussion of the result.

S.S. Alexandrova – conducted the experiments.

A.A. Selivanov – performed *X*-ray diffraction analysis.

A.N. Bykadorov – conducted experiments and contributed to the discussion of the results.

D.A. Prokopenko – prepared the initial samples.

Вклад авторов

А.А. Ашмарин – проведение рентгенофазового анализа.

М.И. Гордеева – участие в обсуждении результатов.

С.Я. Бецофен – участие в обсуждении результатов, написание статьи.

А.А. Лозован – определение цели работы, участие в обсуждении результатов, написание статьи.

R. Wu – участие в обсуждении результатов.

С.С. Александрова – проведение экспериментов.

А.А. Селиванов – проведение рентгеноструктурного анализа.

А.Н. Быкадоров – проведение экспериментов, участие в обсуждении результатов.

Д.А. Прокопенко – приготовление исходных образцов.

The article was submitted 29.06.2023, accepted for publication 04.07.2023

Статья поступила в редакцию 29.06.2023, подписана в печать 04.07.2023